Journal of Macromolecular Science, Part A
Publication details, including instructions for authors and subscription information:
http://www.informaworld.com/smpp/title~content=t713597274

Water Sorption Properties and Antimicrobial Action of Zinc Oxide Nanoparticles-Loaded Cellulose Acetate Films

V. Chaurasia[a]; Navin Chand[b]; S. K. Bajpai[a]
[a] Polymer Research Laboratory, Department of Chemistry, Govt. Model Science College (Auton.), Jabalpur, M.P., India [b] Scientist Grade "G" and Head, Polymer Composites and Chairman Academic Committee (AMPRI), Advanced Materials and Processes Research Institute (Formerly RRL Bhopal), Bhopal, M.P., India

Online publication date: 12 February 2010

To cite this Article Chaurasia, V. , Chand, Navin and Bajpai, S. K.(2010) 'Water Sorption Properties and Antimicrobial Action of Zinc Oxide Nanoparticles-Loaded Cellulose Acetate Films', Journal of Macromolecular Science, Part A, 47: 4, 309 — 317
To link to this Article: DOI: 10.1080/10601320903539207
URL: http://dx.doi.org/10.1080/10601320903539207

Journal of Macromolecular Science, Part A: Pure and Applied Chemistry (2010) **47**, 309–317

ISSN: 1060-1325 print / 1520-5738 online
DOI: 10.1080/10601320903539207

Taylor & Francis
Taylor & Francis Group

Water Sorption Properties and Antimicrobial Action of Zinc Oxide Nanoparticles-Loaded Cellulose Acetate Films

V. CHAURASIA[1], NAVIN CHAND[2] and S.K. BAJPAI[1,*]

[1]*Polymer Research Laboratory, Department of Chemistry,Govt. Model Science College (Auton.), Jabalpur (M.P.)-482001 India*
[2]*Scientist Grade "G" and Head, Polymer Composites and Chairman Academic Committee (AMPRI), Advanced Materials and Processes Research Institute (Formerly RRL Bhopal), Bhopal (M.P.), India*

Received, Accepted September 2009

In this work, ZnO nanoparticles loaded cellulose acetate (ZOLCA) films have been prepared and characterized by XRD, SPR and SEM analysis. The moisture permeation properties of the films have been investigated. The GAB isotherm model has been found to fit well on the moisture uptake data obtained at different temperatures. The monolayer sorption capacity χ_m was found to decrease from 0.059 to 0.0079 g water/g dry film with increase in temperature from 20 to 37°C. The isosteric heat of sorption, when studied in the lower water activity range of 0.04 to 0.10, was evaluated to be 46.55 to 87.29 kJ/mol. The water vapor permeability across the ZOLCA films was found to increase with temperature and activation energy of moisture sorption process was found to be 48.57 kJ/mol. These films have shown excellent antibacterial action against model bacteria *E-Coli* when investigated by qualitative and quantitative methods. Films exhibit great potential to be used as edible films to protect food stuff against microbial infections.

Keywords: Edible films, cellulose acetate, nanoparticles, *E-Coli*, GAB isotherm

1 Introduction

Antimicrobial packaging is a fast developing technology that can be employed to control the microbiological decay of perishable food products (1). Different organic and inorganic active antimicrobial agents can be incorporated into the film matrices to prevent undesirable microbial spoilage occurring during storage of packaged fresh food (2). Although, most films used to preserve food stuff have been produced from synthetic polymers; nevertheless, for environmental reasons, attention has been focused lately on natural biopolymers such as polysaccharides (3–6), proteins (7–9) and lipids (10) or the combination of these components for the preparation of food packaging films. These films are usually loaded with antimicrobial agents which, on coming in contact with food stuff, act upon food born microorganisms and inhibit their growth. These agents belong to a wide spectrum of organic/inorganic compounds (11), essential oils (12), bacteria-originated antibacterial protein (bacteriocins) (13), enzymes (14), fruit extracts (15) etc. Although, these antibacterial agents have shown great potential in inhibiting microbial growth in food stuff, the development of new strains of bacteria that are resistant to current antibiotics (16) has become a serious problem in public health. Therefore, the current research has been focused on the search for new bactericides that can effectively reduce the harmful effects of microorganisms. With the emergence of nanotechnology, the search for effective biocidal agents has been concentrated on the development of nanostructure of coinage metals like silver, copper, zinc and gold (17). Recently, there have been several reports regarding the antimicrobial activity of ZnO nanoparticles (18). It has been reported, on the basis of preliminary growth analysis, that ZnO nanoparticles have higher antibacterial affects on microorganism like *S. Aureus* than other metal oxide nanoparticles (19). Similarly, Tam et al. (20) have reported antibacterial activity of ZnO nanorods prepared by hydrothermal method. ZnO exhibited fair activity against *E. Coli* and *B. Atrophaeus*, but it was considerably more effective in the later case (at 15 mM vs. 5mM concentration respectively, showing zero viable cell count). For both organisms, damage of cell wall was observed. Recently, Padmavathy et al. (21) have prepared ZnO nanoparticles of different sizes and characterized them by SEM, TEM and XRD analysis. It was observed that nano ZnO showed enhanced antibacterial activity as compared to bulk ZnO which is attributed to the generation of reactive oxygen species (ROS) on the surface of ZnO nano particles. ROS are species such as superoxide, hydroxyl radical etc. which are actively involved in damage of bacterial

*Address correspondence to: Dr. S. K. Bajpai, Polymer Research Laboratory, Department of Chemistry, Govt. Model Science College (Auton.), Jabalpur (M.P.)-482001 India. E-mail: sunil.mnlbpi@gmail.com; navinchand15@yahoo.co.in

cells. In the present study, cellulose acetate films loaded with ZnO nanoparticles have been prepared and investigated for antibacterial action against *E.coli*. To the best of our knowledge, this is the first study involving nano ZnO-loaded cellulose acetate films as a food packaging material. Zinc is a good choice in food contact applications for the following reasons. It is an essential micronutrient and serves an important and critical role in our growth and development. Zinc is available in different forms for supplementation and for fortification (22). Zinc oxide has been used in food stuff. It decomposes into Zn (II) ions after entering the body (23). It is also used in the food industry (24).

2 Experimental

2.1 Materials

Cellulose acetate (CA; almost 80% acetylated as per manufacturers' specifications), zinc chloride, sodium hydroxide, and solvent dimethylformamide (DMF) were purchased from Hi Media Laboratories, Mumbai, India and used as received. Nutrient agar, agar-agar type I and nutrient broth were received from S. D. Fine Chemicals, Mumbai, India. Different salts, used to prepare saturated solutions to provide desired relative humidity (RH), were also obtained from E-Merck, Mumbai, India. The Milli-pore water (conductivity 0.06–0.10 μS/cm and bacterial count <10 CFU/ml) was used throughout the investigations.

2.2 Preparation of Zinc Oxide Loaded Cellulose Acetate (ZOLCA) Films

The ZOLCA film was prepared by *in situ* formation of zinc oxide within the cellulose acetate film using the hydrothermal approach. In brief, to a 0.2 percent (w/v) solution of cellulose acetate in DMF, a precalculated amount of $ZnCl_2$ was added and the resulting solution was transferred into teflon coated petri dishes and kept in an electric oven (Tempstar, India) at 80°C for a period of 12 h. The film, thus formed, was peeled off and put in a 0.02M solution of sodium hydroxide. After 4 h, the film was taken out and kept in an electric oven at 70°C for complete conversion of $Zn(OH)_2$ into ZnO. Finally, the film was washed with distilled water and dried in a dust free chamber at ambient temperature until it was completely dry. Similarly, plain cellulose acetate (PCA) film was also prepared.

2.3 Film Characterization

The morphological features of plain and ZnO loaded films were observed using a JOEL JSM840A (Japan) scanning electron microscope. DSC analysis was performed with a Metter DSC-30 thermal analyzer with PCA and ZOLCA. Film of known weight (ca 2.4 mg) was taken in a sealed aluminum pan and the sample was heated from 40°C to 260°C at the heating rate of 10°C per minute under the constant flow of argon gas. The X-ray diffraction pattern (XRD) of nano ZnO was analyzed with a PANalytical X'pert PRO MPD^{R}X-ray diffractometer. The UV-Visible spectrum of the nano ZnO dispersed in distilled water was recorded in a UV-Visible spectrophotometer (Shimadzu 6300) in the range of 300–550 nm. The zinc oxide (ZnO) nanoparticles were prepared by the wet chemical method using zinc nitrate and sodium hydroxide as precursors. Zinc nitrate, 14.874 g (0.1 mol), was dissolved in 500 ml of distilled water under vigorous stirring to ensure complete dissolution. After complete dissolution, 0.2 mol of sodium hydroxide solution was added under constant stirring, drop by drop touching the walls of the vessel. The reaction was allowed to proceed for 2 h after complete addition of sodium hydroxide. The solution was then allowed to settle overnight and supernatant was discarded carefully. The remaining solution was centrifuged at 200 rpm for 10 min and the supernatant was discarded. The residual mass was dried at 80°C for overnight. During drying, complete conversion of $Zn(OH)_2$ into ZnO took place. A 0.2% (w/v) solution was used to record UV-Vis spectrum.

2.4 Moisture Content Studies

The moisture sorption isotherms were determined gravimetrically using the static method as described by Alhamdan et al. (25). Pre-weighed films were placed in Petri dishes inside glass desiccators containing different saturated salt solutions, thus providing a constant relative humidity environment ranging from 3 to 98% as described elsewhere (26). The desiccators were placed inside a temperature-controlled incubator (Tempstar India), set at a desired temperature. The samples were weighed at different time intervals using an electronic balance (Denver Germany) with an accuracy of 0.0001 g. Equilibrium was considered to have been obtained when three consecutive measurements were identical. The equilibrium moisture contents were calculated on a dry basis from which moisture sorption isotherms were drawn.

2.5 Water Vapor Permeability (WVP) Measurement

Water vapor transmission of film was measured using the ASTM E 96–93 method (27). The test cups were filled with 20 g of silica gel (desiccant) to produce a 0% RH below the film. A sample was placed in between the cups and the silicon coated ring cover and held with four screws around the cups' circumference. The air gap was at approximately 1.5 cm in between the film surface and desiccant. The water vapor transmission rate (WVTR) of each film was measured at 100% RH and 25 $\pm$1°C. After taking initial weight of the test cup, it was placed in glass desiccators containing distilled water to provide100% RH. The cups were taken out at different time intervals and weighed accurately. Three replicates of each sample were measured.

The water transmission rate (WVTR) and other related parameters were calculated (28):

$$\text{WVTR} = \frac{\Delta W}{\Delta t.A}\ gs^{-1}m^{-2} \quad (1)$$

$$\text{Permeance} = \frac{\Delta W}{\Delta t.A.\Delta P}\ gs^{-1}m^{-2}Pa^{-1} \quad (2)$$

$$\text{Permeability} = \frac{\Delta W.\chi}{\Delta t.A.\Delta P}\ gs^{-1}m^{-1}Pa^{-1} \quad (3)$$

where $\Delta W/\Delta t$ = amount of water transmission per unit time,
χ = film thickness,
A = surface area of the film exposed to water vapor
ΔP = water vapor pressure difference across the film,

2.6 Antibacterial Studies

Antibacterial studies of zinc oxide loaded cellulose acetate film were carried out quantitatively and qualitatively by the, killing kinetics, viable cell count method (29), and zone inhibition method (30), respectively, with *E. Coli* as the model bacteria.

For the killing kinetics method, each film was cut into a square shape (1 cm × 1 cm). These samples were then immersed in 20 ml nutrient broth in a 25 ml universal bottle. The medium was inoculated with 200 μl of *E.Coli* in its late exponential phase, and then transferred to an orbital shaker and rotated at 37°C at 200 r.p.m. The culture was sampled periodically during the incubation to obtain microbial growth profiles. The same procedure was repeated for the control plain cellulose acetate film. The optical density was measured at 610 nm. The O.D values were converted into concentrations of *E. coli* colony forming units (CFU) per ml using the approximation that an O.D value of 0.1 corresponded to a concentration at 10^8 cells per ml.

In the cell count method, a 100 μl sample of bacterial suspension cultured in nutrient broth (with a concentration of 10^5or10^7 CFU/ml of *E.coli*) was plated on definite quantity of finely cut pieces of film and the plates were incubated at 37°C . The number of resultant colonies was counted after 24 h of incubation. All the experiments were done in triplicate and average data were produced.

In the zone inhibition method one hundred micro liters of the inoculums solution was added to 5 ml of the appropriate soft agar, which was sprayed onto hard agar plates. Circular disks were cut from the test films (diameter = 3.0 cm) and were placed on the bacterial lawns. The plates were incubated for 48 h at 37°C in the appropriate aerobic incubation chamber. The plates were visually examined for zones of inhibition around the film disc and diameter of the zone was measured at two cross-sectional points and the average was taken as the inhibition zone.

3 Results and Discussion

3.1 Formation of ZOLCA Film

The *in situ* formation of ZnO nanoparticles within the cellulose acetate film is a relatively newer technique developed by us with the major objective of getting almost uniform distribution of ZnO nanoparicles within the film matrix. The overall scheme for formation of ZOLCA film may be given as follows: When zinc chloride and cellulose acetate are dissolved in DMF, the Zn (II) ions bind with electron rich species, like oxygen atoms, present in the cellulose acetate molecules in the dissolved state. Later on, when the film is allowed to be dried at 80°C, the film matrix has almost uniformly distributed Zn (II) ions bound to oxygen atoms. Finally, when the film is put in aqueous solution of sodium hydroxide, the OH^- ions enter into the network and cause precipitation of $Zn(OH)_2$ which, on thermal curing, yields ZnO nanoparticles. Here, it is also worth mentioning that since thermal dehydration of $Zn(OH)_2$ precipitate yields ZnO particles, there is the chance of formation of relatively larger sized particles, as also confirmed by SEM analysis.

3.2 Characterization of ZOLCA Film

The surface plasmon resonance (SPR) is a characteristic of metal nanoparticles. The room temperature UV-Vis absorbance spectrum for the ZnO particles has been shown in Figure 1. The sharp absorbance peak, located at about 362 nm, corresponds to the band gap of 3.42 eV. This is almost in accordance with the value of bulk ZnO (31), thus suggesting excellent crystal quality of the ZnO nanoparticles. Therefore, no blue shift was observed in UV-Vis spectrum, revealing that nanoscale ZnO particles obtained are not small enough to show quantum confinement related effects.

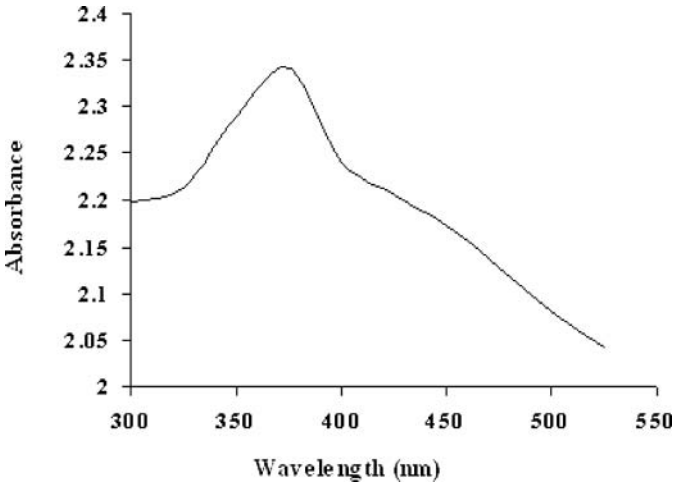

Fig. 1. Surface Plasmon Spectrum for ZnO nanoparticles.

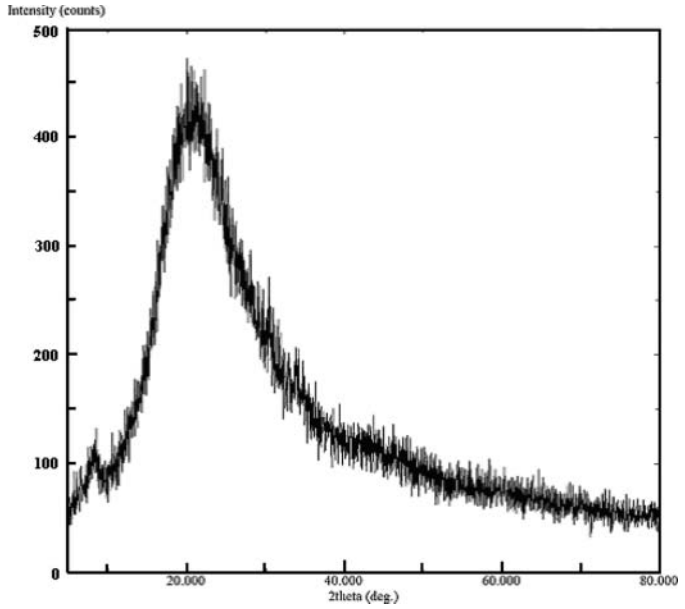

Fig. 2. X-ray diffraction pattern for ZnO nanoparticles loaded cellulose acetate film.

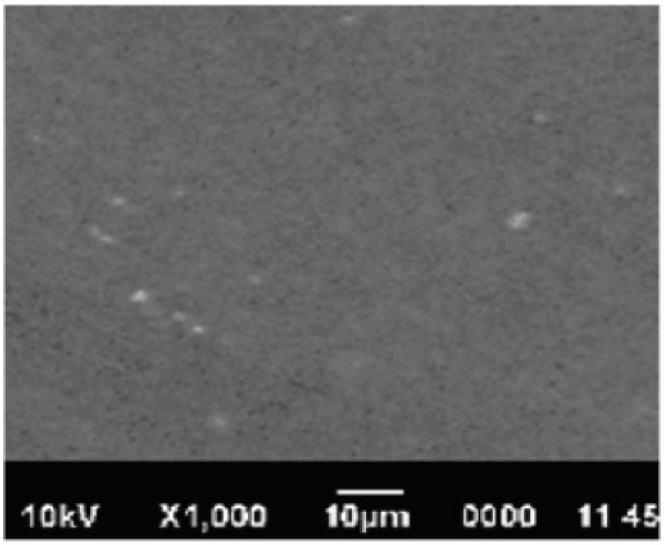

(A)

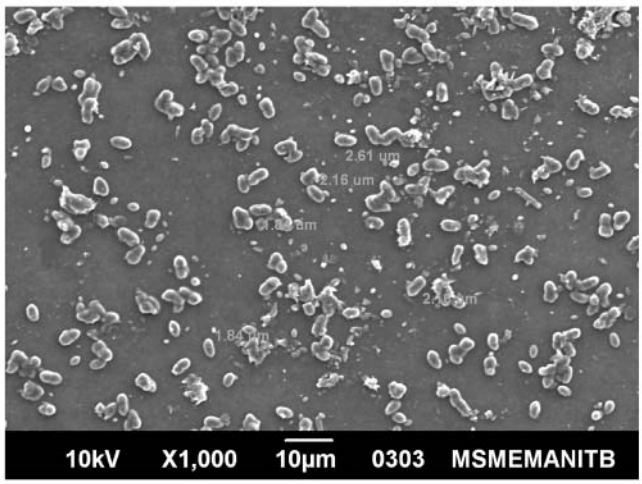

(B)

Fig. 3. SEM images for (A) Plain and (B) Zinc oxide nanoparticles loaded film.

An asymmetric tail can also be found on higher wavelength of the peak, induced by light scattering.

XRD pattern of ZnO nanoparticles-loaded cellulose acetate film is shown in Figure 2. The diffractogram exhibits a broad peak at 2θ value of 22.5° which confirms the presence of cellulose acetate matrix (32). The nano sized ZnO particles are of wurtzite structure (hexagonal face, space group $P6_3mc$). All the diffraction peaks can be well indexed to the hexagonal phase ZnO reported in JCPDS (i.e., Joint Comittees on Power Diffraction Standards) card (No. 36–1451, a = 0.3249 nm, c = 0.5206 nm). The peaks obtained at 2θ value of 31.76, 34.42, 36.25, 47.53, 56.60, 62.86,67.96 and 69.10 correspond to reflection at (100), (002), (101), (102), (110), (103), (112) and (201) respectively. Similar results have been reported elsewhere (33). Here, it is to be noted that some additional peaks were also observed that would be attributed to the presence of impurities.

Scanning electron microscopy (SEM) is an effective tool to study the surface morphology of materials. Figure 3 (A) and (B) give a comparative depiction of the SEM images of plain cellulose acetate and zinc oxide loaded cellulose acetate (ZOLCA) films respectively. It is quite evident from Figure 3(A) that PCA film exhibits smooth surface while the surface of ZOLCA film , as shown in Figure 3(B), demonstrates crystalline structure of ZnO nanoparticles in an almost uniformly distributed manner. The average size of the ZnO nanoparticles was found to be approximately 1200 nm which, in fact, lies far away from the prescribed size of nanoparticles (34).

The differential scanning colorimetry (DSC) offers useful information about crystallinity of a polymeric material (35). In a semi-crystalline polymer like cellulose acetate, the crystalline melting transition, T_m renders valuable information about degree of crystallinity of the polymer. Figure 4(A) and (B) show DSC thermograms of plain and nano ZnO loaded cellulose acetate films, respectively. Sharp endothermic peaks, observed in both the curves indicate crystalline melting transition (T_m) of the polymeric films. It can be seen that values of T_m for PCA and ZOLCA films are nearly 139 and 130°C, respectively thus suggesting a slight decrease in crystalline melting transition due to incorporation of nano zinc oxide particles within the film matrix. This may simply be explained as follows: The incorporation of ZnO nanoparticles within the film matrix causes a decrease in the degree of crystallinity of the polymer matrix, thus resulting in decrease in crystalline melting transition (i.e., T_m) of the polymeric film. Here, it is also worth

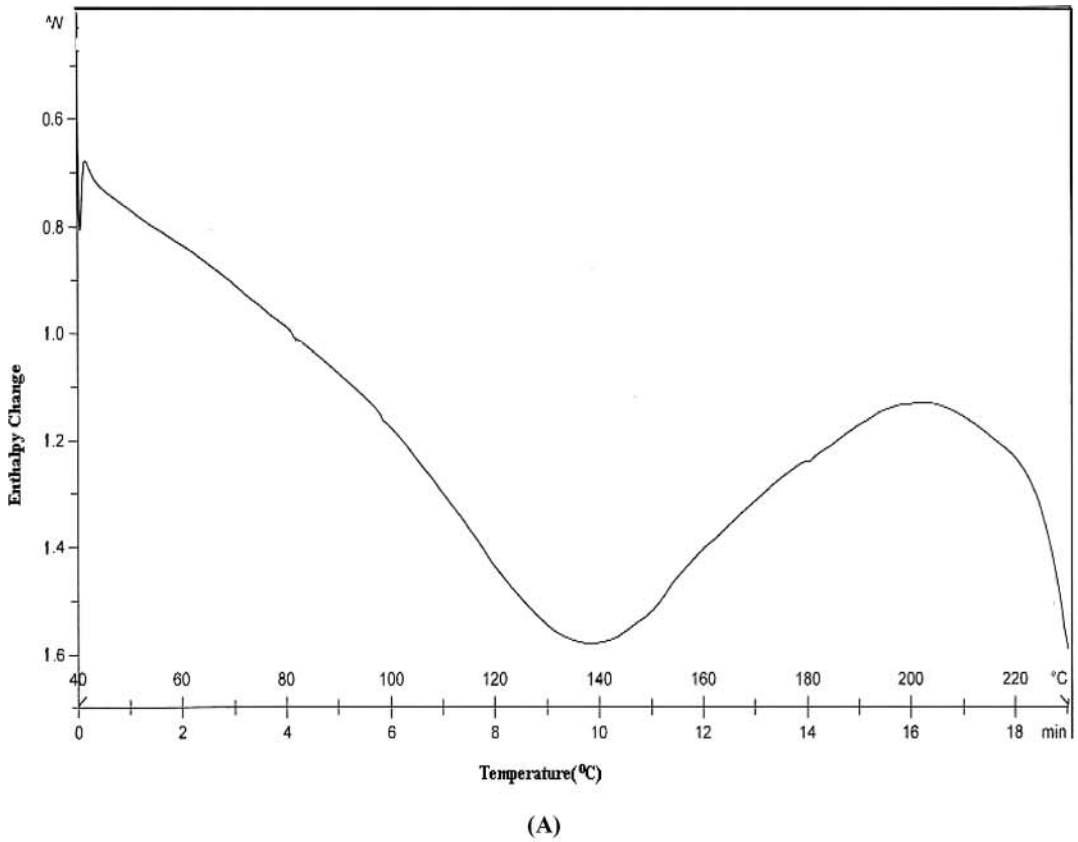

(A)

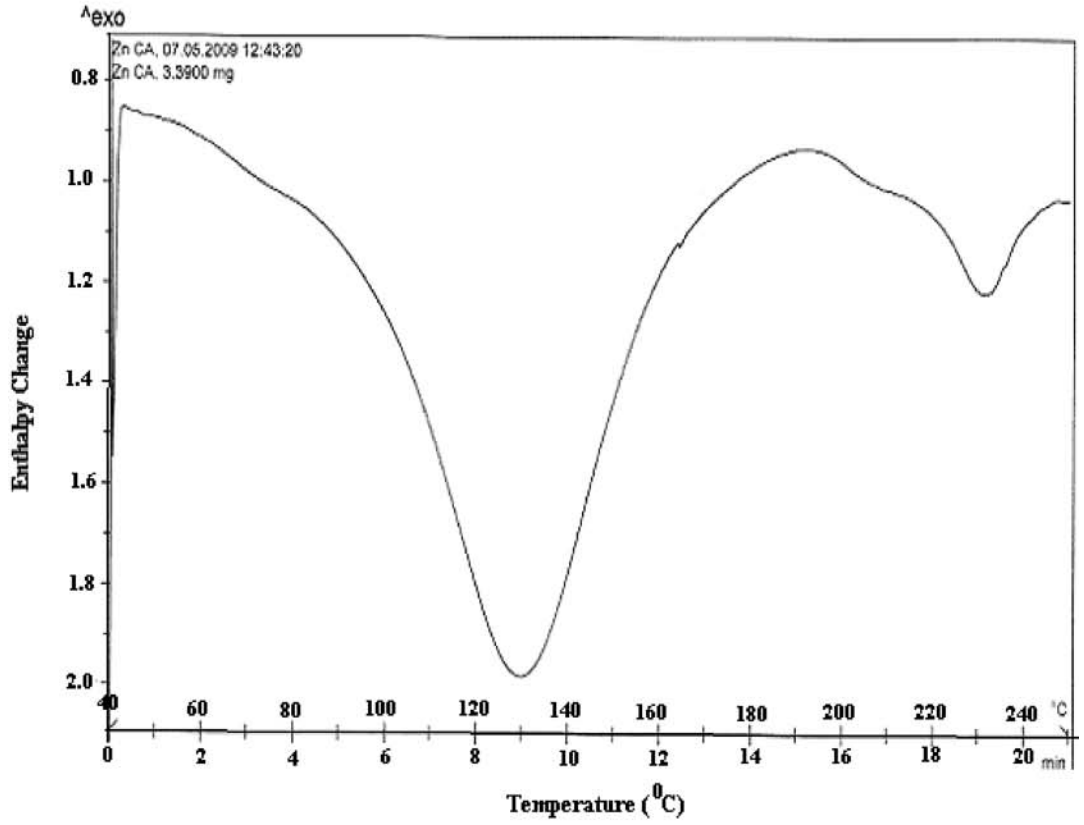

(B)

Fig. 4. DSC thermograms for (A) plain cellulose acetate and (B) ZOLCA films.

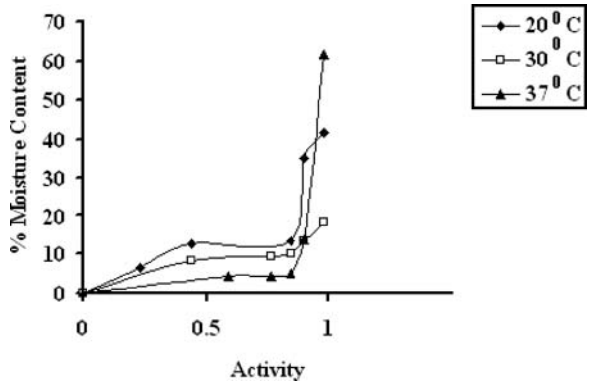

Fig. 5. Isotherm of ZOLCA films at 20°C, 30°C, and 37°C.

mentioning that Kwon et al. (36) have also suggested that metal compounds act as plasticizer or impurities and increase the mobility of the polymer chains, thus resulting in a decrease in their crystalline character.

3.3 Moisture Sorption Isotherms

Water vapor pressure and temperature are the most significant factors determining the moisture uptake properties of a food packaging film. In fact, higher moisture content considerably restricts its use as potential packaging material. The equilibrium moisture content of zinc oxide loaded cellulose acetate (ZOLCA) films was investigated in the environment of varying relative humidity (RH) at 20, 30, and 37°C. The sorption isotherms, as displayed in Figure 5, show typical sigmoidal shape, thus confirming class II classification in which the polymer absorbs relatively smaller quantity of water at lower water activities and larger amount at higher relative humidity (37).The explanation for the nature of the isotherm may be that, at low water activities, physical sorption on active sites of film occurs only on the surface. However, in the intermediate water activity range, sorption takes place at less active sites also. It is also clear from Figure 5 that the moisture content of film does not increase with increasing temperature at any given RH. At lower RH (activity), e.g., 0.5, equilibrium moisture content decreases with increasing temperature. This may simply be attributed to the fact that as the temperature increases, water vapor molecules possess more kinetic energy and hence, show less tendency to get sorbed onto ZOLCA film, thus causing a decrease in moisture uptake. Similar type of behavior has also been reported earlier by other workers (38). Hence, moisture content uptake may be regarded as an exothermic process.

The equilibrium moisture sorption data, obtained at three temperatures, was applied on a well known GAB isotherm model (39), given as:

$$X = \frac{X_m C K a_w}{[(1 - K a_w + C K a_w)]} \tag{4}$$

Where X is the moisture content sorbed pre g of film, X_m is the moisture content sorbed on monolayer, C and K are sorption constants related to temperature as shown by the following expressions:

$$C = C_G \exp \frac{(\Delta H_C)}{RT} \tag{5}$$

$$K = K_G \exp \frac{(\Delta H_K)}{RT} \tag{6}$$

Where ΔH_c and ΔH_k are functions of heat of sorption of water; C_G and C_K are adjusting constants for the temperature effect, and T is the absolute temperature. The values of X_m, as determined using non-linear regression analysis, were found to be 0.059, 0.026 and 0.007 g water/g dry film at 20, 30 and 37°C, respectively. The monolayer moisture content X_m is recognized as the moisture content affording the longest time period with minimum quality loss at a given temperature. Therefore, at a given temperature, the safest water activity level is that corresponding to X_m or lower. Finally, it is assumed that strong sorbent-sorbate interactions, which are exothermic, are favored at lower temperature, thus causing a decrease in GAB constant C (40) which is in accordance with Equation 1 that describes the temperature dependence of C. In our study, the value of C were found to be nearly 85.17, 1.60, and 0.60 at 20, 30 and 37°C, respectively, thus showing complete agreement with the temperature dependency of C as indicated by Equation 5. It is also worth mentioning here that there is a sharp decrease in values of C when the temperature increases from 20 to 30°C, thus indicating that strong sorbate-sorbent interaction is favored at 20°C, whereas a poor interaction is observed at 30 to 37°C. Therefore, it may be inferred that the use of packaging film in the vicinity of 30°C shall be more beneficial.

3.4 Isosteric Heat of Sorption (q_{st})

The net isosteric heat of sorption, q_{st}, is a good measure of the interaction of water vapor with the solid substrate. It is also known as binding energy of sorption and defined as the difference $q_{st} - \Delta H_{vap}$where q_{st} is the total heat of sorption and ΔH_{vap} is heat of vaporization of water at a given temperature (41). Thus, it may be considered as indicative of intermolecular attractive forces between the sorption sites and water vapor molecules.

The integrated form of the Clausius-Clapeyron equation, correlating water activity as a function of temperature, can be given as:

$$\ln a_w = \frac{-q_{st}}{RT} + C \tag{7}$$

Where q_{st} is the net isosteric heat of sorption (kJ mol^{-1}), R is gas constant (R = 8.314 kJ $mol^{-1}K^{-1}$) and C is a constant.

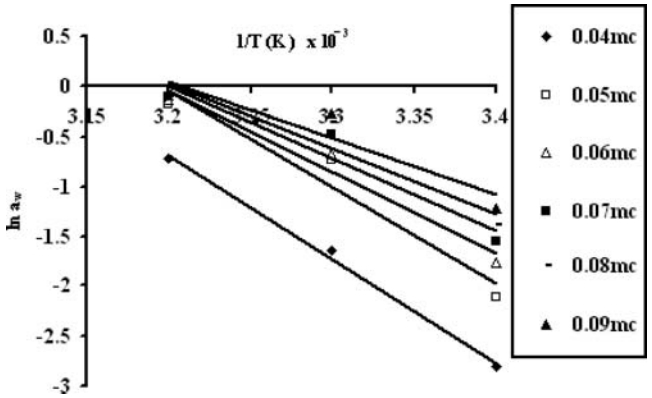

Fig. 6. Water activity vs. reciprocal of temperature plots for plain cellulose acetate film to determine $q_{st.}$

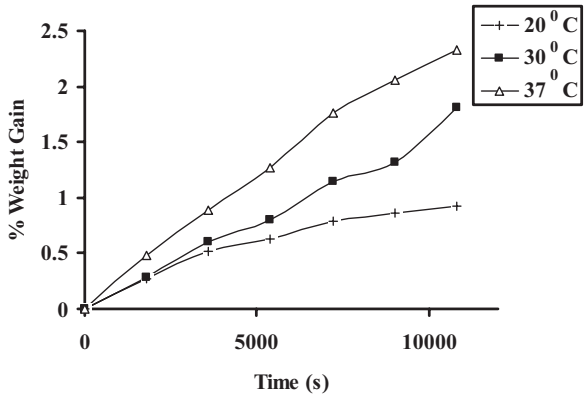

Fig. 8. Kinetics of water vapor transmission through ZOLCA film at different temperatures.

Water activity was plotted against the reciprocal of absolute temperatures at various moisture contents as shown in Figure 6. The sorption isosteors showed smooth straight lines thus confirming that Equation 7 fit the experimental data. For the moisture content range of 0.05 to 0.10, the net q_{st}values were obtained in the range of 46.55 to 87.29 kJ/mol. The values obtained indicate that q_{st}values are large at low moisture content and decrease with an increase in moisture content. The observed positive values of q_{st}suggest an easy physical sorption of water molecules forming a mono molecular layer. Finally, the q_{st} values, as a function of moisture content are shown in Figure 7. It is clear that q_{st} values decrease with an increase in moisture content. This may be attributed to the fact that initially sorption occurs on the most active available sites, giving rise to high interaction energy. As these sites become occupied, sorption occurs on the less active site, thus giving rise to lower heat of sorption. At low moisture content, the higher heat of sorption could be due to strong interaction between water molecules and remaining –OH groups of cellulose acetate molecules.

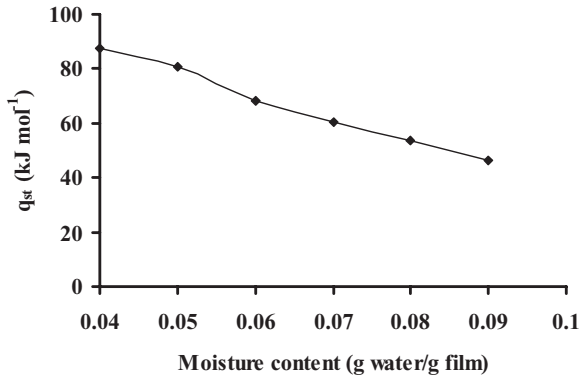

Fig. 7. Variation in values of $q_{st}$with moisture content.

3.5 WaterVapor Permeation Studies

Since the main function of an edible film or coating is often to impede moisture transfer between food and the surrounding atmosphere, or between two components of a heterogeneous food product, water vapor permeability (WVP) should be minimum. The variation of WVP with temperature is usually given by an Arrhenius type equation (42) as shown below:

$$\mathrm{WVP} = \mathrm{WVP}_0 \exp^{\frac{-E_p}{RT}} \tag{8}$$

Where Ep is the apparent activation energy for the permeation phenomenon ($kJmol^{-1}$). The nano zinc oxide loaded cellulose film was placed under relative humidity of 100% at three different temperatures, namely 20, 30 and 37°C, and was investigated for moisture permeation through films. The results, as shown in Figure 8, clearly show that the amount of water vapor permeated through films increases with temperature. This may simply be attributed to the enhanced movements of polymeric segments of film and also due to increased kinetic energy of the permeating water vapor molecules. The dynamic uptake data was also used to determine various kinetic parameters which are given in Table 1. Finally, in order to determine the activation energy E_a, ln WVP values were plotted against 1/T, which yielded straight line (data not displayed). The slope of the linear plot was used to calculate E_a, which was found to be nearly 48.57 kJ/mol.

Table 1. Kinetics of permeability of zinc oxide nano-loaded cellulose acetate film at different temperatures

	Temperatures		
Parameters	*20°C*	*30°C*	*37°C*
WVTR ($gs^{-1}m^{-2}$)	0.175	0.350	0.526
Permeance ($gs^{-1}m^{-2}Pa^{-1}$)	2.79×10^{-5}	5.59×10^{-5}	8.38×10^{-5}
Permeability ($gs^{-1}m^{-1}Pa^{-1}$)	1.11×10^{-9}	2.23×10^{-9}	3.35×10^{-9}

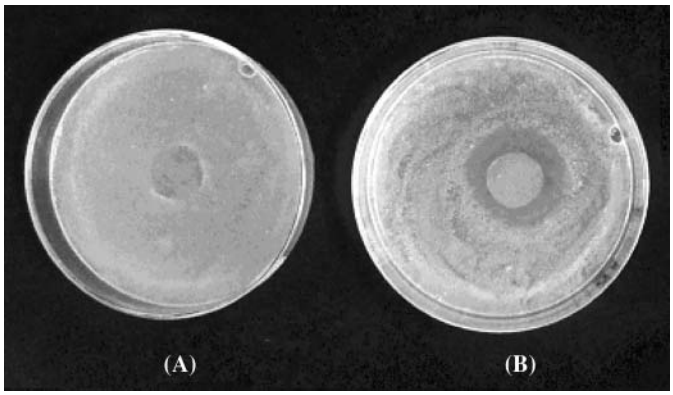

Fig. 9. Evaluation of antibacterial action for (A) Plain Cellulose Acetate, and (B) ZOLCA films by 'zone inhibition' method.

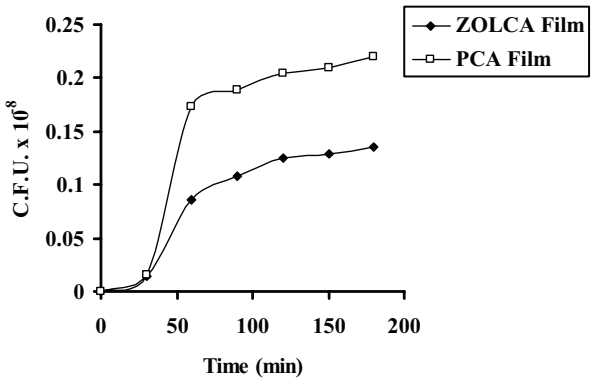

Fig. 11. Kinetics of bacterial growth for plain cellulose acetate and ZOLCA films against *E. coli*.

3.6 Antibacterial Investigations

The antibacterial action of ZOLCA film was tested against *E-Coli* as model bacteria, taking plain cellulose acetate (PCA) film as control. The results of investigations have been well depicted in Figure 9. It is clear from Figure 9(A) that there is dense population of bacterial cells in the petri plate supplemented with PCA film while a clear zone of inhibition appears surrounding the circular piece of ZOLCA film in the petri plate as shown in Figure 9(B). Moreover, we also cut film into small pieces and spread over the whole petri plate. The results, as shown in Figure 10, reveal that the plate, supplemented with pieces of ZOLCA (Fig. 10(B)) film shows less dense population of bacterial cells while the plate containing pieces of plain film, has dense colonies of bacterial cells (Fig. 10(A)). The number of bacterial colonies was found to be approximately 2112 vs. 3848 for control set. Therefore, it is clear that zinc oxide nanoparticles loaded cellulose acetate film has the potential to inhibit bacterial colonies.

We also studied the 'killing kinetics' of bacterial cells in liquid NB medium. Figure 11 shows a comparative depiction of time-dependent growth of bacterial colonies in nutrient broth supplemented with pieces of plain, as well as nanozinc oxide loaded, films. The results reveal that the growth rate of bacterial colonies is suppressed to a great extent in the NB which contains pieces of nanozinc oxide loaded film. On the other hand, there is sharp increase in the number of bacterial cells in NB containing pieces of plain cellulose acetate film. Therefore, it may be concluded that zinc oxide nanoparticles loaded cellulose acetate film has great potential to be used for inhibition of microbial growth in foodstuff.

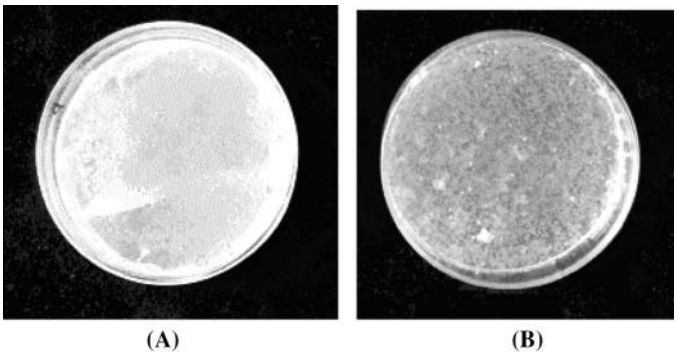

Fig. 10. Number of colonies grown in petri-plates supplemented with (A) Plain cellulose acetate and (B) ZOLCA films.

4 Conclusions

From the above study, it may be concluded that ZnO nanoparticles loaded cellulose acetate film can be used as edible film to restrict moisture permeation, as well as bacterial growth in food products.

References

1. Conte, A., Singaglia, M. and Del Nobile, M.A. (2007) *J. Dairy Sci.*, 90, 2126–2131.
2. Ahn, J., Grun, I.U. and Mustapha, A. (2004) *J. Food Protection*, 67(1), 148–155.
3. Vargas, M., Albors, A., Chiratt, A. and Gongalez Martinez, C. (2009) *Food Hydrocolloids*, 23(2), 536–547..
4. The, D. Phan., Debeaufort, F., Voilley, A. and Luu, D. (2009) *J. Food Engineering*, 90(4), 548–558.
5. Bourtoom, T. and Chinnan, M. S. (2008) *LWT Food Science and Technology*, 41, 1633–1641.
6. Bertuzzi, M.A., Castro Vidaurre,E.F., Armada, M. and Gottifredi, J. C. (2007) *J. Food Engineering*, 80, 972–978.
7. Perez-Mateas, M., Montero, P. and Gomez-guillen, M. C. (2009) *Food Hydrocolloids*, 23:53–61.
8. Sivarooban, T., Hettiarachchy, N. S. and Johnson, M.G. (2008) *Food Res. International*, 41, 781.
9. Del Nobile, M.A., Conte, A., Incoronato, A.L. and Panza, O. (2008) *J. of Food Engineering*, 98, 57–63.
10. Suppakul, P., Miltza, J., Sonneveld, K. and Bigger, S.W. (2003) *J. of Food Science*, 68(2), 408–420.
11. Eswaranandam, S., Hettiarachychy, N.S. and Johnson,M.G. (2004) *Journal of Food Science*, 69(3), 79–84.

12. Chaibi, A., Ababouch, L.H., Belasri, K., Boucetta, S. and Busta, F.F. (1997) *Food Microbiology*, 14, 161–174.
13. Kim, H., Roh, I., Kim, K., Jang, I., Ha, s., Song, K., Park, S., Lee, W., Youn K. and Bae, D. (2006) *J. Microbiology Biotechnology*, 16(4), 597–600.
14. Gucbilmez, C. M., Yemenicioglu, A. and Arslanoglu, A. (2007) *Food Res. Int*., 40, 80–91.
15. Conte, A., Serpanza, B., Sinigaglia, M. and Del Nobbile, M.A. (2007) *J. Food Protection*, 70(1), 114–118.
16. Singh, M., Singh, S., Prasad, S. and Gambhir, I.S. (2008) *Digest J. Nanometer Biostructures*, 3(3), 115–120.
17. Sondi, I. and Salopek – Sondi, B. (2004) *J Colloids Interface Sci*., 275, 177–182.
18. Yadav, A., Prasad, V., Kathe, A.A., Raj, S., Yadav, D., Sundarmoorthy, C. and Vigneshvaran, N. (2006*) Bull Marter Sci.,* 29(6), 641–645.
19. Jones, N., Ray, B., Ranjit, K.T. and Manna, A.C. (2007) *FEMS Microbiology Letters*, 279, 71.
20. Tam, K.H., Djurisic, A. B., Chan, C.M.N., Xi, Y.Y., Tse, C.W., Leung, Y.H., Chan, W. K. and Leung, F.C.C. (2008) *Thin Solid Films*, 516(18), 6167.
21. Padmawathy, N. and Vijayaraghavan, R. (2008) *Sci. Technology Advanced Material*, 9, 1.
22. Shi, L., Zhou, J. and Gunasekaran, S. (2008) *Material Lett*., 62, 4383–4386.
23. Yu, H.H., Shan, Y.S. and Li, P.W. (2007) *Formosan J. Med. Assoc*., 106, 864–867.
24. Hotz, C. and Brown, K.M. (2004) *Food Nutr. Bull*., 25, 595–603.
25. Alhamdan, A. M. and Hassan, B. H. (1999) *J. Food Engineering*, 39, 301–322.
26. Oluwamukomi, M.O., Adeyemi I.A. and Odeyemi, O.O. (2008) *Agricultural Engineering Int*., 10, 1–10.
27. ASTM Standard Test Method for Water Vapor Transmission of Materials Designation E, 1993, 701:93–96.
28. Bozdemir, O.A. and Tutas, M. (2003) *Turk. J. Chem*., 27, 773–782.
29. Pal, S., Tak, Y.K. and Song, J.M. (2007) *Appl. Environ. Microbiol*., 73(6), 1720.
30. Qin, Y., Zhu, C., Chen, Y. and Zhang, C. (2006) *J. Appl. Polymer Sci*., 101, 766–771.
31. Yang, P.D., Yan, H. Q., Mao, S., Russo, R., Jhonson, J. and Saykally, R. (2002) *Adv. Funct. Mater*, 12, 323–331.
32. Valente, A.J.M., Burrows, H.D., Polishchuk, A.Y., Dominggues, C.P., Bores, O.M.E., Eusebio, M.E. S., Maria, T.M.R., Lobo, V.M.M. and Monakman, A.P. (2005) *Polymer*, 46, 5918–5928.
33. Chen, C., Liu, P. and Lu, C. (2008) *Chemical Eng. J*., 144, 509–513.
34. Bajpai, S.K., Murali Mohan, Y., Bajpai, M., Tankhiwale, R. and Thomas, V. (2007) *J. Nanoscience and Nanotechnology*, 7(9), 1–17.
35. Goula, A.M., Karapantsios, T.D., Achilias, D.S. and Adamopoulos, K.G. (2008) *J. Food Eng.*, 85, 73–83.
36. Kwon, J., Yoon, S.H., Lee, S.S. and Shim, H. (2005) *Bull Korean Chem. Soc*., 26(5), 837–840.
37. Al-Mutaseb, A.H. (2004) *J. Food Eng.,* 64, 107–113.
38. Goula, A.T., Karapantsios, T.D., Achilias, D.S. and Adamopoulos, K.G. (2008) *J. Food Eng*., 85, 73–83.
39. Venden Berg, C. and Bruin, S. Water Activity and its Estimation in Food Systems: Theoretical Aspects, In: 'Water Activity: Influence of Food Quality', Rockland, L.B. and Stewart, G.F. (Eds), Academic Press: New York, 1981, pp 1–61.
40. Gabas, A.L., Telis, V.R.N., Sobral, P.J.A. and Telis-Romero, J. (2007) *J. Food Eng*., 82, 246–252.
41. Napierala, D.M. and Nowotarska, A. (2006) *Acta Agrophysica*, 7(1), 151–159.
42. Kester, J.J. and Fennema, O. (1989) *J. Food Sci*., 54, 1383–1389.